JOURNAL OF MATERIALS SCIENCE **36** (2001) 771–777

Mechanical properties of cement foams in shear

JONG-SHIN HUANG*, KWAN-DER LIU
Department of Civil Engineering, National Cheng Kung University, Tainan, 70101 Taiwan
E-mail: jshuang@mail.ncku.edu.tw

Existing models indicate that the mechanical properties of brittle foams in shear depend on relative density, cell size, cell geometry and the modulus of rupture of solid cell walls. A series of mechanical testing on alumina cement foams with various relative densities were conducted to measure their shear modulus, shear strength and fracture toughness. Experimental data are compared to the existing theoretical models. Results suggest that the existing models for closed-cell foams are applicable to describe the mechanical properties of alumina cement foams in shear. Also, the microstructure coefficients included in the theoretical expressions for mechanical properties of alumina cement foams have been determined.

1. Introduction

Sandwich structures with metal or plywood faces and cementitious foam cores have been commercially available for a number of years in construction. The separation of two faces by a lightweight foam core significantly increases the bending and buckling resistance of sandwich structures with little increase in weight. Both the stiffness and loading capacity of sandwich structures, however, become lower as the relative density of foam cores decreases. When both lightweight and high loading capacity are sought in a design of sandwich structures, faces are typically much thinner, stiffer and stronger than cores. As a result, faces primarily carry bending moment exerted on sandwich structures while cores are mainly loaded by shear force. Therefore, the structural integrity of sandwich structures, especially used for load-bearing components, is strongly affected by the mechanical properties of lightweight foam cores in shear.

Cement foams are preferably used as core materials for sandwich structures in building construction because they have low thermal conductivity, good fire resistance and high melting temperature compared to polymeric foams. However, lightweight cement foams with high porosity possess relatively lower stiffness and strength. The bending rigidity and loading capacity of sandwich structures are thus controlled by the mechanical properties of cement foams. Since lightweight cores are normally subjected to in-plane shear stresses, the shear modulus and strength of cement foams play an important role in determining the rigidity, loading capacity and corresponding failure mode of sandwich structures. At the same time, pre-existing cracks or flaws in brittle cement foams resulting from manufacturing or machining might cause catastrophic failure of sandwich structures. Presumably, the crack surface within cement foams may not be exactly perpendicular to the imposed in-plane shear stresses, leading to a tensile (mode I), shearing (mode II) or mixed-mode fracture. Hence, the brittle fracture for cement foams under mode I or mode II loading needs to be fully investigated to determine the possibility and direction of crack propagation in sandwich structures.

The literature on the mechanical properties of cement foams is limited. Short and Kinniburgh [1] reported some testing results on Young's modulus and compressive strength of cement foams. They found that the mechanical properties of cement foams decrease as the relative density decreases. Tonyan and Gibson [2] presented the microstructural characterization and elastic properties of Portland cement foams with a relative density ranging from 0.1 to 0.45. Large coalesced voids were observed from image analysis and attributed to the coalescence of individual cells into larger voids within foamed cement matrix. The measured elastic moduli and compressive strengths of Portland cement foams were analyzed by using a combination of a cell-wall-bending model and some empirical equations for porous solids. However, no attempt has been made to study the mechanical properties of Portland cement foams in shear. Huang and Huang [3] gave some experimental results on compressive fatigue of alumina cement foams. It was found that the number of cycles to failure for alumina cement foams increases with increasing relative density but with decreasing cyclic stress range.

In this paper, microstructure characterization and mechanical testing on alumina cement foams are first conducted. Resulting measurements of cell length, shear modulus, shear strength, mode I and mode II fracture toughness for alumina cement foams with various relative densities will be compared to existing theoretical models. Consequently, the complete theoretical expressions describing the mechanical properties of alumina cement foams in shear are obtained.

* Author to whom all correspondence should be addressed.

2. Existing models

Gibson and Ashby [4] proposed a cubic cell model to analyze the linear elastic properties of closed-cell foams. They suggested that mechanical property for a closed-cell foam is the sum of three contributions: cell-edge bending, cell-face stretching and cell-fluid compression. For closed-cell cement foams, the contribution of cell-fluid compression can be neglected because the cell fluid is air instead of liquid. Thus, the theoretical expression for shear modulus of closed-cell cement foams, G^*, is:

$$\frac{G^*}{G_s} = C_1\left(\phi\frac{\rho^*}{\rho_s}\right)^2 + C_1''(1-\phi)\frac{\rho^*}{\rho_s} \qquad (1)$$

where ϕ is the volume fraction of solid contained in the cell edges, $(1-\phi)$ is the remaining fraction of solid contained in the cell faces, and G_s is the shear modulus of solid cell walls. The relative density, ρ^*/ρ_s, is the density of foams, ρ^*, divided by the density of solid material from which they are made, ρ_s. The microstructure coefficients C_1 and C_1'' were found to be 1.0 [4] while Demsetz and Gibson [5] found that C_1 is 1.44 for rigid polyurethane foams.

When brittle cement foams are under in-plane shear stresses, the induced bending moment exerted on individual solid cell wall become dominant as compared to the induced axial and shear forces if the relative density is relatively low. As a result, brittle rupture failure of solid cell walls is more likely to occur. The maximum applied in-plane shear stresses at which the extreme fiber tensile stress of individual solid cell wall reaches their modulus of rupture, σ_{fs}, can be calculated by using dimensional argument analysis as suggested by Gibson and Ashby for foamed materials [4]. When the cell-wall modulus of rupture is assumed to be constant, the theoretical expression for shear strength of brittle closed-cell foams, τ^*, can be expressed as:

$$\frac{\tau^*}{\sigma_{fs}} = C_2\left(\phi\frac{\rho^*}{\rho_s}\right)^{3/2} + C_2''(1-\phi)\frac{\rho^*}{\rho_s} \qquad (2)$$

Here C_2 and C_2'' are another microstructure coefficients. The values of $C_2 = 0.2$ and $C_2'' = 1.0$ are obtained from the cubic cell model [4]. Triantafillou and Gibson [6] measured the shear strengths of rigid polyurethane foams and found that C_2 is 0.31.

Using the singular tensile stress field near macrocrack tip of a continuum model, Maiti *et al.* [7] were able to derive the theoretical expression for mode I fracture toughness of open-cell foams as a function of cell size ℓ, relative density and the cell-wall modulus of rupture. The mode I fracture toughness of closed-cell foams, K_{IC}^*, is affected by both cell-edge bending and cell-face stretching. The argument parallels that used for shear modulus and shear strength, giving:

$$\frac{K_{IC}^*}{\sigma_{fs}\sqrt{\pi\ell}} = C_3\left(\phi\frac{\rho^*}{\rho_s}\right)^{3/2} + C_3''(1-\phi)\frac{\rho^*}{\rho_s} \qquad (3)$$

Again, C_3 and C_3'' are microstructure coefficients and C_3 was experimentally determined to be 0.65 [7].

Similarly, Huang and Lin [8] utilized the near-tip singular in-plane shear stresses to calculate the critical bending moment exerted on the first unbroken cell wall ahead of the macrocrack tip. The mode II fracture toughness was obtained from the maximum applied in-plane shear stresses at which the first unbroken cell wall will fracture. The theoretical expression for mode II fracture toughness of brittle closed-cell foams can be written in a similar form:

$$\frac{K_{IIC}^*}{\sigma_{fs}\sqrt{\pi\ell}} = C_4\left(\phi\frac{\rho^*}{\rho_s}\right)^{3/2} + C_4''(1-\phi)\frac{\rho^*}{\rho_s} \qquad (4)$$

Here C_4 and C_4'' are another microstructure coefficients and can be determined empirically.

The existing models suggest that the mechanical properties of brittle closed-cell foams in shear depend on relative density, cell size, cell geometry and the material properties of solid cell walls (G_s and σ_{fs}). A series of mechanical tests are needed to determine the corresponding microstructure coefficients in the theoretical expressions and to verify the validity of the existing models for alumina cement foams with different relative densities.

3. Experimental methods

3.1. Processing and preparation of specimens

The required constituents for producing cement foam specimens are alumina cement (Asano, Japan), water, superplasticizer and preformed air bubbles. The chemical composition of alumina cement is listed in Table I. A foaming agent (provided by Elastizell, U.S.A.) diluted with water in a 1 : 30 solution was pressurized in a tank to generate preformed air bubbles. Alumina cement slurry with a water/cement ratio of 0.6 and with a superplasticizer/cement ratio of 0.005 was made first. The relative densities of alumina cement foams were controlled by the method of adding different amounts of preformed air bubbles into alumina cement slurry; the density of the solid alumina cement is 1780 Kg/m^3. In the study, five different design relative densities of alumina cement foams were considered: 0.18, 0.22, 0.3, 0.4 and 0.5.

A mechanical processing method of mixing preformed air bubbles with alumina cement slurry was utilized to produce alumina cement foam specimens. After complete mixing of alumina cement slurry and preformed air bubbles, the wet cement foam was cast into steel molds. 24 hours later, the alumina cement foam specimens were removed from steel molds and

TABLE I The chemical composition of alumina cement used for producing foam specimens

Composition	Weight Fraction (%)
SiO_2	5.0
Al_2O_3	53.0
Fe_2O_3	0.8
CaO	38.2
TiO_2	2.3

cured in water at a temperature of 25°C. After 7 days of hardening, the alumina cement foam specimens were trimmed on both ends and then air dried for an additional 2 days. The volume and weight of each alumina cement foam specimen were recorded to calculate its actual relative density.

3.2. Microstructural characterization

The wet alumina cement foams were poured along the gravitational direction into cubic steel molds with a dimension of 50 mm × 50 mm × 50 mm. In order to characterize the cell length distribution in three principal directions for each cubic specimen, two mutually perpendicular sections were cut and observed. The two sections of each specimen were trimmed first, and then scanned and analyzed by the image analysis software Adobe Photoshop on a personal computer. The contrast-enhanced, darkened and enlarged digital images of the scanned sections were utilized to characterize the cell length distributions in three principal directions. The cell lengths along three principal directions, ℓ_1, ℓ_2 and ℓ_3, for alumina cement foam specimens were measured and their number fractions obtained from the scanned cut-sections were counted over 500 cells and recorded.

3.3. Mechanical tests

A wave-velocity measurement apparatus (Sonic Viewer 170, Japan) was used to determine the dynamic shear modulus for alumina cement foam specimens with different relative densities. Transducers were mounted on both ends of each alumina cement foam cylinder with a diameter of 75 mm and a height of 150 mm. The velocity of impulse waves through the tested cylinder can be recorded and converted to the dynamic shear modulus of each alumina cement foam specimen. Dynamic shear moduli of 3 specimens were measured and averaged for each relative density of alumina cement foams. The dynamic shear modulus of solid alumina cement was also measured.

Cylindrical specimens with a diameter of 63.5 mm and a height of 20 mm were produced to measure the shear strength of alumina cement foams using a direct shear tester (ELE, U.K.). The required specimen dimension and loading configuration for the direct shear test are illustrated in Fig. 1. During each direct shear testing, a constant compressive normal force should be imposed to ensure a shear failure of alumina cement foam specimens. Three different compressive normal forces of 45.6, 65 and 105 N were used for each relative density of alumina cement foams. Direct shear tests were performed at a constant horizontal displacement rate of 0.5 mm/min up to shear failure, at which a peak shear force is obtained. The peak shear forces of 3 specimens for each compressive normal force were measured and averaged. Then, the measured peak shear forces for specimens under three different compressive normal forces were extrapolated to get the peak shear force for specimens under no compressive normal forces. The shear strength of alumina cement foams was calculated from the extrapolated peak shear force divided by their horizontal cross-sectional area.

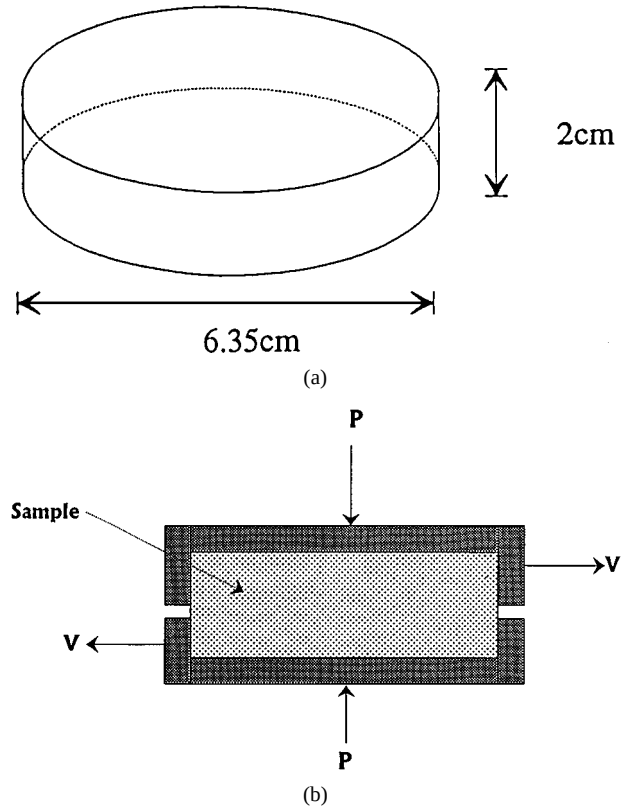

Figure 1 The specimen dimension and loading configuration for the direct shear test.

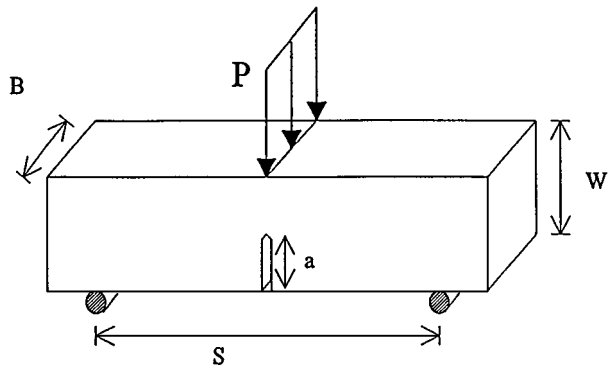

Figure 2 The specimen geometry and loading configuration of a three-point bend test for measuring the mode I fracture toughness of alumina cement foams.

Beam specimens of 40 mm × 50 mm × 210 mm were produced for testing mode I fracture toughness. A central saw-cut notch was made for each beam specimen loaded in three point bending. Ten notched specimens were tested at each relative density. Fig. 2 shows the specimen geometry and loading configuration of the three-point bend test. The crosshead of an Instron machine moved at a constant speed of 0.5 mm/min. The load and deflection were recorded on a computer up to the point at which fracture occurred. The mode I fracture toughness for each specimen was calculated from the applied load at failure.

Short beam shear specimens of 50 mm × 50 mm × 100 mm were made and used to measure the mode II fracture toughness of alumina cement foams. Two saw-cut notches with a depth of 25 mm were made for each short beam shear specimen. Fig. 3 shows the specimen

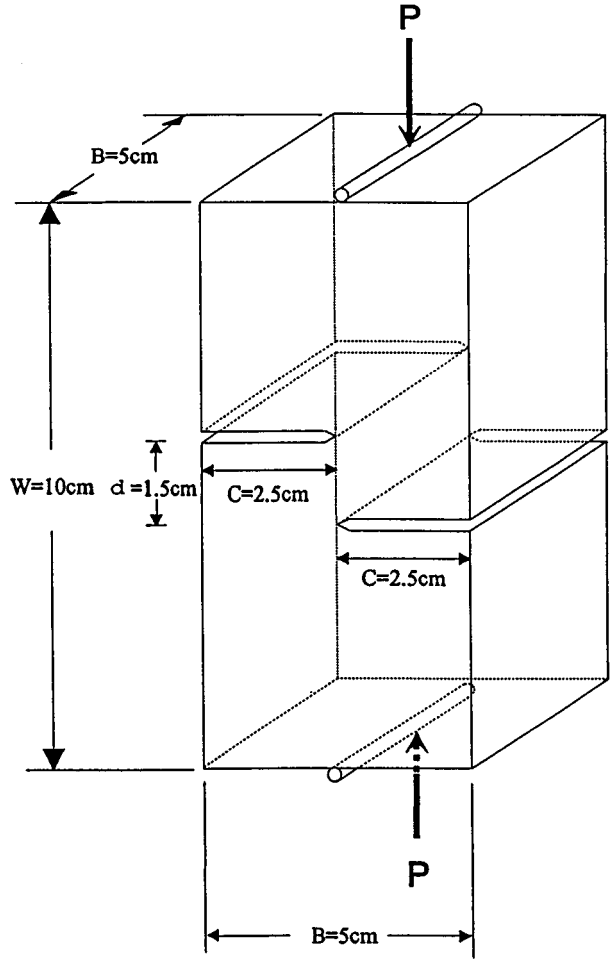

Figure 3 The specimen geometry and loading configuration of a short beam shear test for measuring the mode II fracture toughness of alumina cement foams.

geometry and loading configuration of the short beam shear test. Ten specimens were tested at each relative density. The crosshead moved at a constant speed of 0.5 mm/min. Again, the mode II fracture toughness for each specimen was calculated from the applied load at failure.

4. Results and discussion

4.1. Microstructural characterization

The measured cell lengths ℓ_1, ℓ_2, ℓ_3 and their distributions for alumina cement foams with various relative densities are presented in Figs 4–6, respectively; ℓ_3 is along the gravitational direction while ℓ_1 and ℓ_2 are normal to the gravitational direction. Note that no large coalesced voids as reported by Tonyan and Gibson [2] in their Portland cement foams have been observed in alumina cement foams. Since the scanned sections of alumina cement foam specimens provide the two-dimensional cell lengths, a correction factor is needed to estimate the true three-dimensional cell lengths. The measured two-dimensional cell lengths from the scanned sections are converted to the three-dimensional cell lengths by multiplying a factor of $4/\pi$ as suggested by DeHoff and Rhines [9] for spherical particles with a uniform size. The resulting mean cell lengths in the three principal directions for alumina cement foams with different relative densities are listed in Table II. From Figs 4–6, it can be said that the cell structure within alumina cement foams is approximately axisymmetric due to the effect of gravitational loading of solid cell walls. The aspect ratios for the axisymmetric closed-cells within alumina cement foams are calculated and listed in Table II.

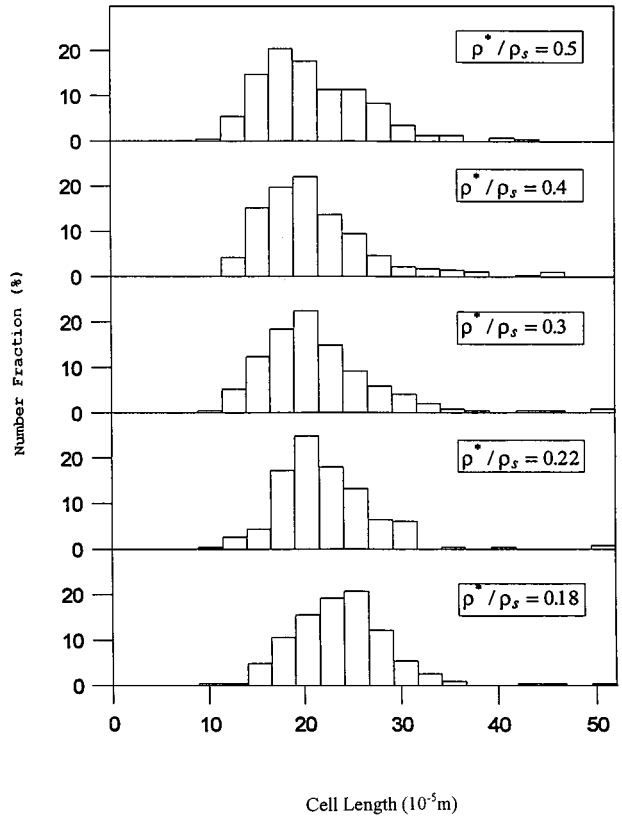

Figure 4 The measured cell lengths ℓ_1 and their distributions for alumina cement foams with various relative densities.

4.2. Mechanical tests

The dynamic shear modulus of solid alumina cement is 4.72 GPa. The measured dynamic shear moduli of alumina cement foams with different relative densities as shown in Fig. 7 can be described by the following equation:

$$\frac{G^*}{G_s} = 0.64\left(\frac{\rho^*}{\rho_s}\right)^2 + 0.22\frac{\rho^*}{\rho_s} \qquad (5)$$

Equation 5 represents the theoretical model for $C_1 = 1.0$, $C_1'' = 1.1$ and $\phi = 0.8$ in Equation 1; that is,

TABLE II Mean cell lengths in three principal directions and aspect ratios for alumina cement foams with different relative densities

	Relative density (ρ^*/ρ_s)				
	0.5	0.4	0.3	0.22	0.18
Mean cell lengths:					
$\bar{\ell}_1$ (μm)	268.8	269.4	272.4	279.7	304.7
$\bar{\ell}_2$ (μm)	265.2	266.8	270.3	274.9	307.9
$\bar{\ell}_3$ (μm)	228.3	235.1	240.0	249.7	267.2
Aspect ratios:					
$\bar{\ell}_3/\bar{\ell}_1$	0.849	0.873	0.881	0.892	0.877
$\bar{\ell}_2/\bar{\ell}_1$	0.987	0.990	0.993	0.983	1.010

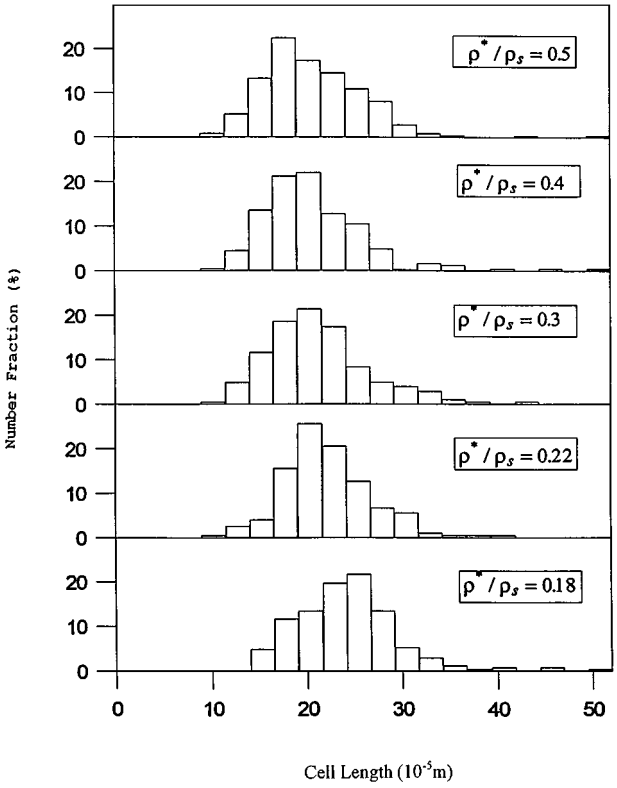

Figure 5 The measured cell lengths ℓ_2 and their distributions for alumina cement foams with various relative densities.

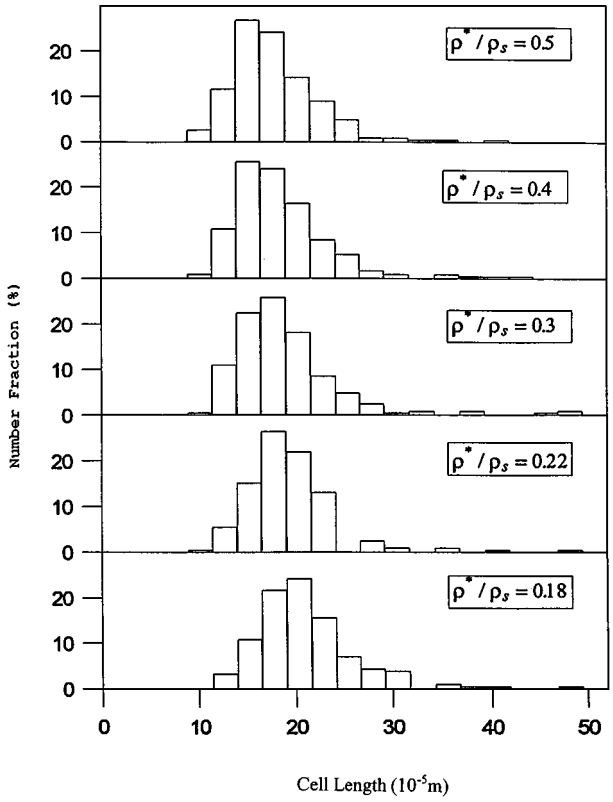

Figure 6 The measured cell lengths ℓ_3 and their distributions for alumina cement foams with various relative densities.

80% of solid alumina cement paste is contained in the cell egdes. The microstructure coefficients C_1 and C_1'' are close to the theoretical value of 1.0 as suggested by Gibson and Ashby for closed-cell foams [4].

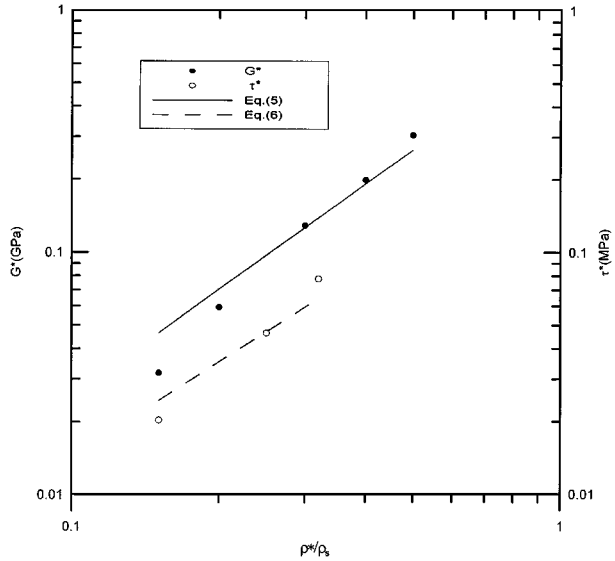

Figure 7 The dynamic shear moduli and shear strengths of alumina cement foams with different relative densities.

Experimental results on the shear strengths of alumina cement foams are also shown in Fig. 7. Only specimens with lower relative densities (0.18, 0.22 and 0.3) were tested due to the limitation of shearing capacity of 2KN allowable for the direct shear tester. The relation between shear strength and relative density for alumina cement foams is obtained as follows:

$$\frac{\tau^*}{\sigma_{\mathrm{fs}}} = 0.14\left(\frac{\rho^*}{\rho_{\mathrm{s}}}\right)^{3/2} + 0.12\frac{\rho^*}{\rho_{\mathrm{s}}} \tag{6}$$

From the above equation, $C_2 = 0.2$, $C_2'' = 0.6$ and $\phi = 0.8$ are found for the theoretical model of Equation 2. The microstructure coefficient $C_2'' = 0.6$ is smaller than 1.0 as suggested by Gibson and Ashby for crushing strength of closed-cell foams [4].

The crack depth for notched beam specimens under three point bending (Fig. 2) is 20 mm, giving the ratio of the crack depth to the cell length greater than 10 as recommended by Huang and Gibson [10] to eliminate the short crack effect on foamed materials. The mode I fracture toughness of notched alumina cement foam specimens loaded in three point bending can be calculated from the applied concentrated force at failure, P, using the equation proposed by Srawley [11]:

$$K_{\mathrm{IC}}^* = \frac{PS}{BW^{3/2}} f\left(\frac{a}{W}\right) \tag{7}$$

Where S, B, W and a are the span, width and depth of notched specimens and the notch depth, respectively, as illustrated in Fig. 2; the dimensions of notched beam specimens are $W = 4$ cm, $B = 5$ cm, $a = 2$ cm and $S = 16$ cm. The function $f(a/W)$ is given by the following equation:

$$f\left(\frac{a}{W}\right) = \frac{3\left(\frac{a}{W}\right)^{0.5}\left\{1.99 - \frac{a}{W}\left(1-\frac{a}{W}\right)\left[2.15 - 3.93\left(\frac{a}{W}\right) + 2.7\left(\frac{a}{W}\right)^2\right]\right\}}{2\left(1+2\frac{a}{W}\right)\left(1-\frac{a}{W}\right)^{1.5}} \tag{8}$$

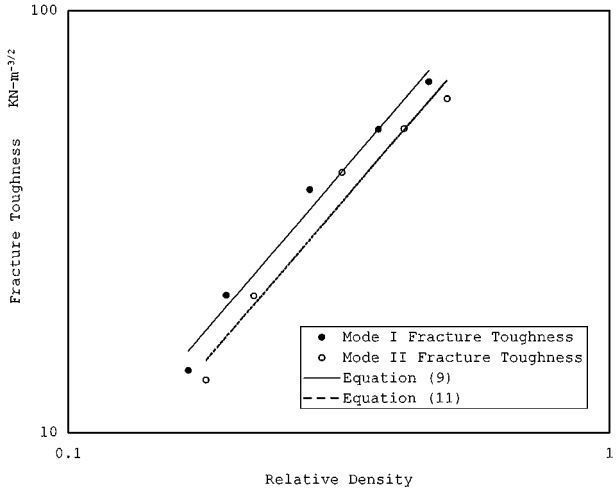

Figure 8 The measured mode I and II fracture toughnesses of alumina cement foams.

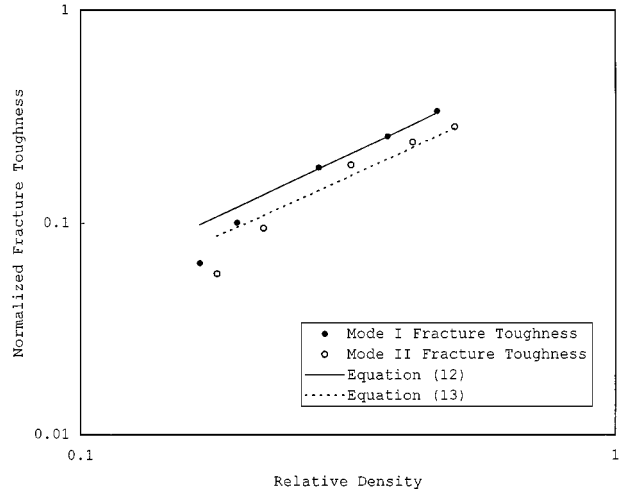

Figure 9 The normalized mode I and II fracture toughness for alumina cement foams with different relative densities.

The mode I fracture toughness for the notched beam specimens of varying relative density are shown in Fig. 8. The measured mode I fracture toughnesses of alumina cement foams can be described well by the equation:

$$K_{\mathrm{IC}}^{*} = 230.81\left(\frac{\rho^{*}}{\rho_{\mathrm{s}}}\right)^{1.505} \tag{9}$$

Here K_{IC}^{*} has the unit of KN-m$^{-3/2}$.

The mode II fracture toughness of alumina cement foams can be calculated from the applied load at failure, P, in the short beam shear testing by using the equation proposed by Watkins and Liu [12]:

$$K_{\mathrm{IIC}}^{*} = 0.22\frac{P}{Bd}\sqrt{\pi c} \tag{10}$$

Here c, d and B are the notch depth, notch distance and specimen width, respectively, as defined in Fig. 3. The measured mode II fracture toughness of alumina cement foams shown in Fig. 8 fits well with the following equation:

$$K_{\mathrm{IIC}}^{*} = 194.54\left(\frac{\rho^{*}}{\rho_{\mathrm{s}}}\right)^{1.5003} \tag{11}$$

Again, K_{IIC}^{*} has the unit of KN-m$^{-3/2}$. From Fig. 8, it is seen that the mode II fracture toughness is consistently smaller than mode I fracture toughness for alumina cement foams if they have the same relative density.

From Equations 3 and 4, it is known that both the mode I and II fracture toughnesses of alumina cement foams depend on their relative density, cell size and cell-wall modulus of rupture. Cell anisotropy will affect the fracture toughness of alumina cement foams as a function of crack propagation direction, and should be considered here. The pre-cut crack propagates along the gravitational direction for notched beam specimens under three point bend testing while the pre-cut crack propagates normal to the gravitational direction for short beam shear testing. The values of ℓ_3 and ℓ_1 for alumina cement foams with different relative densities can be found from Table II. Also, the modulus of rupture of a solid alumina cement beam ($\rho^{*}/\rho_{\mathrm{s}} = 1$) under three point bending is found to be 6.76 MPa. Since the fracture toughnesses and cell lengths for alumina cement foams have been measured, the microstructure coefficients C_3, C_3'', C_4 and C_4'' can be obtained from experimental results.

When cell anisotropy is taken into account, the normalized mode I fracture toughness of alumina cement foams as shown in Fig. 9 can be rewritten as:

$$\frac{K_{\mathrm{IC}}^{*}}{\sigma_{\mathrm{fs}}\sqrt{\pi\ell}} = 0.46\left(\frac{\rho^{*}}{\rho_{\mathrm{s}}}\right)^{3/2} + 0.40\frac{\rho^{*}}{\rho_{\mathrm{s}}} \tag{12}$$

It is found that $C_3 = 0.65$, $C_3'' = 2.0$ and $\phi = 0.8$ for the theoretical model of Equation 3. At the same time, the normalized mode II fracture toughness of alumina cement foams as shown in Fig. 9 is:

$$\frac{K_{\mathrm{IIC}}^{*}}{\sigma_{\mathrm{fs}}\sqrt{\pi\ell}} = 0.28\left(\frac{\rho^{*}}{\rho_{\mathrm{s}}}\right)^{3/2} + 0.36\frac{\rho^{*}}{\rho_{\mathrm{s}}} \tag{13}$$

From Equation 13, $C_4 = 0.4$, $C_4'' = 1.8$ and $\phi = 0.8$ are found for the theoretical model of Equation 4.

From Fig. 9, it is noted that the measured mode I and II fracture toughness are slightly smaller than those calculated from Equations of 12 and 13 as the relative density of alumina cement foams is decreased. The reason for that might be due to the difficulty of complete mixing of cement slurry and preformed air bubbles as the relative density becomes smaller, introducing some flaws and cracks within solid cell walls. In addition, the coalescence of preformed air bubbles into larger cells for lower relative-density cement foams might produce some flaws and cracks within solid cell walls. As a result of those, the cell-wall modulus of rupture is expected to be smaller, giving a lower fracture toughness.

5. Conclusions

The cell geometry of alumina cement foams is axisymmetric due to the loading of gravitational force of solid cement paste; the cell length along the gravitational direction is shorter than the cell lengths normal to the gravitational direction. Also, no large coalesced voids have been observed within alumina cement foams. Experimental results suggest that the existing models for closed-cell foams are applicable to describe the shear modulus, shear strength and fracture toughness of alumina cement foams. Mode II fracture toughness is consistently smaller than mode I fracture toughness for alumina cement foams. Meanwhile, the microstructure coefficients included in the theoretical expressions for the shear modulus, shear strength, fracture toughness of alumina cement foams have been determined.

Acknowledgement

The financial support of the National Science Council, Taiwan, R.O.C., under contract numbers NSC 83-0410-E006-035, NSC 83-0618-E006-037 is gratefully acknowledged.

References

1. A. SHORT and W. KINNIBURGH, "Lightweight Concrete," 3rd ed. (Applied Science, London, 1978).
2. T. D. TONYAN and L. J. GIBSON, *J. Mater. Sci.* **27** (1992) 6371.
3. J. S. HUANG and Z. H. HUANG, *ibid.*, in press (2000).
4. L. J. GIBSON and M. F. ASHBY, "Cellular Solid: Structures and Properties," 2nd ed. (Cambridge University Press, Cambridge, U.K., 1997).
5. L. A. DEMSETZ and L. J. GIBSON, *Materials Science and Engineering* **85** (1987) 33.
6. T. C. TRIANTAFILLOU and L. J. GIBSON, *ibid.* **95** (1987) 37.
7. S. K. MAITI, M. F. ASHBY and L. J. GIBSON, *Scr. Metall.* **18** (1984) 213.
8. J. S. HUANG and J. Y. LIN, *J. Mater. Sci.* **31** (1996) 2647.
9. R. T. DEHOFF and F. N. RHINES, "Quantitative Microscopy" (McGraw-Hill, New York, 1968).
10. J. S. HUANG and L. J. GIBSON, *Acta Metall. Mater.* **39** (1991) 1627.
11. J. E. SRAWLEY, *Int. J. Frac.* **12** (1976) 475.
12. J. WATKINS and K. L. W. LIU, *International Journal of Cement Composites and Lightweight Concrete* **7** (1985) 39.

Received 7 May 1999
and accepted 28 July 2000